Forest Ecology and Management 448 (2019) 432–444

Contents lists available at ScienceDirect

Forest Ecology and Management

journal homepage: www.elsevier.com/locate/foreco

Coastal Alaska forests under climate change: What to expect?

Wu Ma[a], Xiaoping Zhou[b,1], Jingjing Liang[a], Mo Zhou[a,c,*]

[a] Forest Advanced Computing and Artificial Intelligence Laboratory (FACAI), Department of Forestry and Natural Resources, Purdue University, United States
[b] Pacific Northwest Research Station, Forest Service, United States
[c] School of Natural Resources, West Virginia University, United States

ARTICLE INFO

Keywords:
Matrix growth model
Climate change
Forest dynamics
Disturbances
Temperate rainforest

ABSTRACT

Coastal Alaska forests consist of 2.6 million hectares of productive timberland and constitute the largest terrestrial carbon reservoir in the state. It has become increasingly urgent to understand potential climate-induced changes in forest structural and species composition in this region. Based on in situ data from 544 permanent sample plots (PSPs) for calibration and 244 PSPs for validation, we developed a climate-sensitive density-dependent, species-, and size-specific matrix model (CSMatrix-AK), to predict fine-scale dynamics of coastal Alaska forests from the present to Year 2100 under three climate scenarios – Representative Concentration Pathway (RCP) 4.5, RCP6.0, and RCP8.5. With post-sample validation, we showed that the CSMatrix-AK model was more accurate than other existing models for the region. Under low-intensity and high-frequency stochastic shocks which represented natural disturbances typical for the region, we projected a gradual decline of Sitka spruce, a major commercial species in the region, and a significantly lower level of total stand basal area under all three climate scenarios. The results suggest that timber industry, landowners and managers, policymakers, and local communities will need to prepare for substantial impacts of climate change on Coastal Alaska forests and the regional forestry sector. Our CSMatrix-AK model provides a useful tool to better inform the stakeholders of such changes and lays the foundation for adaptive forest management to sustain forests and associated ecosystem services in the region.

1. Introduction

Coastal Alaska is home to the two largest national forests (NFs) in the United States – Tongass NF and Chugach NF. The 16.7 million-hectare (ha) region is in general recognized as two distinct subregions–southeast and south-central Alaska. Approximately 36 percent of this region is forested (van Hees, 2003), of which 2.4 million-ha is deemed commercially productive (Campbell et al., 2005). The maritime southeast Alaska landscape is characterized by temperate weather and steep slopes, and dominated by shade-tolerant conifers (Ruess et al., 1998). In comparison, a mosaic of boreal and coastal forests occupies different niches over the transitional ecoregion area of south-central region (Nowacki et al., 2003). These coastal forests store the largest amount of terrestrial carbon in the state and are largely in public ownership (Ping et al., 1997). With an abundance of intact old-growth temperate rainforests, this unique region is critical to carbon sequestration, ecological conservation, and economic vitality of local communities. Being part of the climate-change front line due to arctic amplification (Swann et al., 2010), these coastal forests are subject to a greater impact from climate change than the rest of the world, with unprecedented uncertainty in future forest condition, species composition, and attendant ecosystem services.

In coastal Alaska forests, western hemlock (*Tsuga heterophylla)* and Sitka spruce (*Picea sitchensis*) comprise more than 50 percent of total basal area. Shade tolerant mountain hemlock (*Tsuga mertensiana*), Alaska yellow cedar (*Cupressus nootkatensis*), western red cedar (*Thuja plicata*), white spruce (*Picea glauca*), and black spruce (*Picea mariana*) constitute 40 percent of the total basal area (Table 1). Sitka spruce, an important source of sawlogs and fiber, is widely used for construction, pallets/packaging, and fencing, thus playing a critical role in the forest sector of this region (Macdonald and Hubert, 2002). In addition, white spruce has desirable wood machining properties (Hernandez et al., 2001).

Alaska coastal forests provide a wide array of ecosystems services (for a summary see Alaska Coastal Rainforest Center, http://acrc.alaska.edu), which can be categorized as “provisioning, regulating, supporting, and cultural services” (Millenium Ecosystem Assessment, 2005, p.126). Forest industry, as well as fishery and tourism, heavily

* Corresponding author at: Department of Forestry and Natural Resources, Purdue University, 715 W. State Street, West Lafayette, IN 47906, United States.
E-mail addresses: ma628@purdue.edu (W. Ma), mozhou@purdue.edu (M. Zhou).
[1] Retired.

https://doi.org/10.1016/j.foreco.2019.06.030
Received 18 February 2019; Received in revised form 18 June 2019; Accepted 20 June 2019

Table 1
Tree species composition in terms of basal area of 544 calibration plots and 244 validation plots in coastal Alaska forests from the 2014 inventory.

Symbol	Common name	Scientific name	Calibration plots (%)	Validation plots (%)
WH	Western hemlock	*Tsuga heterophylla*	31.21	36.79
SS	Sitka spruce	*Picea sitchensis*	20.06	17.98
MH	Mountain hemlock	*Tsuga mertensiana*	18.34	14.99
AC	Alaska cedars		19.74	20.44
	Alaska yellow cedar	*Cupressus nootkatensis*	11.48	12.68
	Western redcedar	*Thuja plicata*	8.26	7.76
BS	Boreal spruces		2.26	4.36
	White spruce	*Picea glauca*	1.64	3.99
	Black spruce	*Picea mariana*	0.62	0.37
OS	Other species		8.39	5.45
	Lodgepole pine	*Pinus contorta*	3.24	1.92
	Paper birch	*Betula papyrifera*	1.87	1.13
	Black cottonwood	*Populus trichocarpa*	1.31	0.96
	Quaking aspen	*Populus tremuloides*	1.12	0.82
	Red alder	*Alnus rubra*	0.64	0.35
	Subalpine fir	*Abies lasiocarpa*	0.21	0.27
	All Species		100.00	100.00

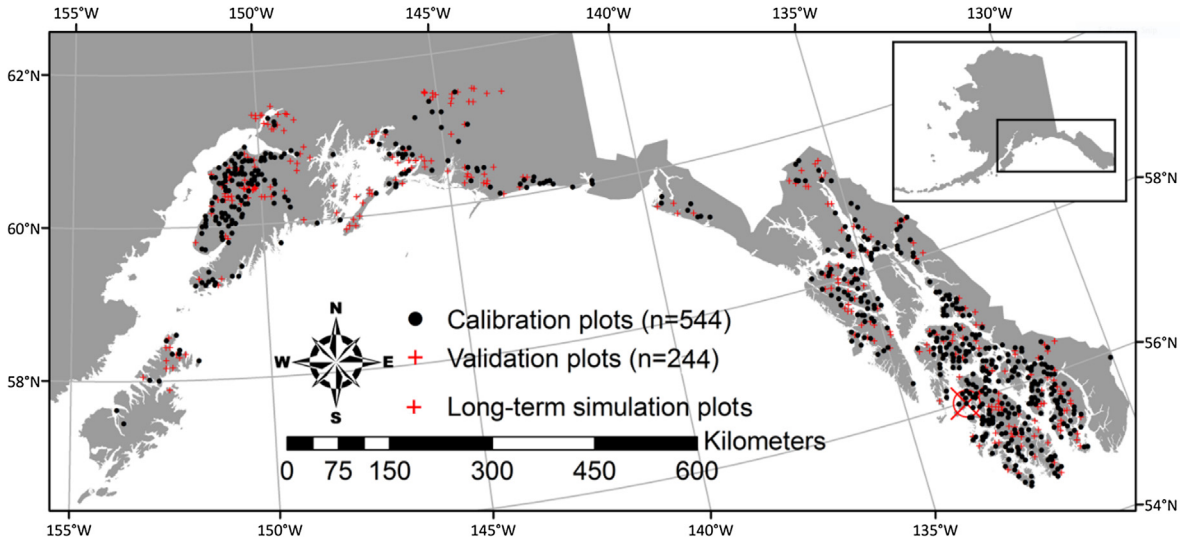

Fig. 1. Geographic distribution of sample plots used to calibrate and validate the matrix growth models. Inset shows the location of the study area within the State of Alaska.

Table 2
Definition and units of variables used in the climate-sensitive matrix model for the Coastal Alaska forests.

Variables	Units	Definition/explanation
a	°	plot aspect in decimal degree
B	$m^2\ ha^{-1}$	total stand basal area
C	$m^3\ ha^{-1}\ yr^{-1}$	site productivity in terms of mean annual increment of volume
D	cm	diameter at breast height
E	10^3 m	plot elevation
g	$cm\ yr^{-1}$	annual diameter growth
H_d	unitless	tree size diversity, measured in Shannon's index
H_s	unitless	tree species diversity, measured in Shannon's index
I	°C	mean growing seasonal temperature
P	10^2 mm	annual total precipitation
m	yr^{-1}	annual tree mortality, the probability that a tree would die within a year
N	$trees\ ha^{-1}$	number of trees per hectare
R	$trees\ ha^{-1}\ yr^{-1}$	recruitment, the number of trees per hectare that grew into the smallest diameter class (12.7–18 cm) in a year
S	°	average slope of each subplot in decimal degree
T	yr	elapsed time between inventories
V	$m^3\ ha^{-1}$	gross single-tree volume

rely on these ecosystem services (Juday et al., 1998). Notwithstanding a historical decline in forest production and employment attributable to controversial forest management plans adopted by the United States (US) Forest Service (Stier, 1980), the coastal region remains the sole area in Alaska where timber harvest revenue offsets new road construction expenses (Berman et al., 1998). Newer policies, such as alternatives to clearcutting (ATC) systems, have been established to stimulate forest industry in this region (McClellan et al., 2000).

Reliable growth and yield (G&Y) estimates are central to informed policy making and conservation and management of the coastal Alaska forests. Previous G&Y tables of the region (Taylor, 1934; Meyer, 1937; Barnes, 1962) are outdated and restrictive (Ritchie, 1999). The two recent models, the Forest Vegetation Simulator- Southeast Alaska Variant (FVS-SEAPROG, Keyser, 2008) and the matrix G&Y model (hereafter, Climate-constant matrix model or CCM, Peterson et al., 2014) have several issues. FVS-SEAPROG, due to insufficient in situ calibration data, was found to underestimate the growth rate of small trees and overestimate that of large trees even in a short timespan (McClellan, 2005; Keyser, 2008). In the long run, such a systematic bias propagates and results in more erroneous forecasts. An earlier matrix model (CCMatrix, Peterson et al., 2014) was developed under the assumption of a constant climate. As climate change affects physiographic conditions, as well as tree growth, productivity, and species distribution in

Table 3
Summary statistics of plot-level variables. *T* and *R* are between the two inventories, and all the remaining variables are at the time of the first inventory. All notations are defined in Tables 1 and 2. SD: standard deviation; Max: maximum value; Min: minimum value.

Variables	Mean	SD	Max	Min	Number of plots
B (m^2 ha^{-1})	32.05	23.08	138.09	0.19	544
C (m^3 ha^{-1} yr^{-1})	2.89	2.45	17.02	0.66	544
H_d	1.66	0.57	2.50	0.00	544
H_s	0.59	0.40	1.45	0.00	544
T (years)	8.03	2.64	13.10	1.00	544
V (m^3 ha^{-1})	271.29	277.06	2,338.49	0.39	544
I (°C)					
WH	12.15	2.31	13.54	−0.61	345
MH	11.66	2.57	12.31	−0.64	260
SS	11.78	2.51	14.44	−1.54	304
AC	12.46	3.04	13.62	3.25	204
BS	12.24	3.36	13.95	−3.53	91
OS	11.88	2.78	14.72	−3.46	203
P (100 mm)					
WH	17.46	7.45	33.05	7.63	345
MH	16.78	6.52	32.45	4.05	260
SS	17.15	7.24	34.24	5.61	304
AC	17.27	7.14	32.54	8.92	204
BS	12.82	4.35	30.25	3.18	91
OS	15.57	5.64	32.96	3.13	203
R (trees ha^{-1} yr^{-1})					
WH	1.17	3.10	34.11	0.00	159
MH	0.88	3.93	45.02	0.00	78
SS	0.39	1.25	11.83	0.00	72
AC	0.42	1.37	13.64	0.00	74
BS	0.95	3.14	26.77	0.00	89
OS	0.56	3.62	69.98	0.00	56
N (trees ha^{-1})					
WH	134.03	168.65	1,323.51	0.00	345
MH	75.80	161.50	1,397.87	0.00	260
SS	60.50	143.64	1,457.35	0.00	304
AC	72.00	131.60	951.74	0.00	204
BS	25.42	83.21	654.32	0.00	91
OS	41.22	80.99	490.74	0.00	203

Table 4
Summary statistics for tree-level variables. All notations are defined in Tables 1 and 2. *D* is calculated at the first inventory, *g* and *m* are calculated between the two inventories. SD: standard deviation; Max: maximum value; Min: minimum value; n: number of trees.

	Species					
	WH	MH	SS	AC	BS	OS
	D (cm)					
Mean	28.11	25.89	31.43	28.13	17.64	23.15
SD	16.51	12.13	19.12	16.75	5.28	9.07
Max	116.33	107.69	147.32	141.47	47.49	67.31
Min	12.70	12.70	12.70	12.70	12.70	12.70
n	4419	2321	1956	2312	713	1256
	g (cm $year^{-1}$)					
Mean	0.11	0.09	0.23	0.09	0.21	0.16
SD	0.18	0.10	0.20	0.11	0.16	0.17
Max	0.64	0.51	1.21	0.58	0.74	0.95
Min	−0.18	−0.24	−0.16	−0.35	−0.24	−0.27
n	4419	2321	1956	2312	713	1256
	m ($year^{-1}$)					
Mean	0.005	0.005	0.006	0.003	0.017	0.008
SD	0.024	0.025	0.027	0.017	0.057	0.025
Max	0.476	1.000	1.000	0.169	0.476	0.476
Min	0.000	0.000	0.000	0.000	0.000	0.000
n	4721	2564	2025	2417	845	1374

the region (Juday et al., 1998), CCMatrix is also subject to a substantial bias, especially in terms of long-term projections.

Climate-sensitive matrix (CSMatrix) models, as an advanced variant of matrix growth models (for a review, see Liang and Picard, 2013), feature a transition matrix calibrated to reflect climatic effects on tree growth, recruitment, and mortality. When paired with disturbance components, CSMatrix models can be extended to simulate vegetation dynamics under risk and uncertainty. For example, Ma et al. (2016) integrate a CSMatrix model with a mean fire interval model to project the dynamics and composition of the U.S. Central Hardwood Forests under changing climate and fire regimes.

The primary objective of this paper is to provide reliable projections of future stand growth, as well as forest stocking and species composition, in coastal Alaska under climate change. To this end, we developed the first climate-sensitive density-dependent, species-, and size-specific matrix model for the coastal Alaska forests (CSMatrix-AK) to project future forests across the region, under three different climate scenarios (i.e. RCP4.5, RCP6.0, and RCP8.5). In addition, our model accounted for small-scale and high-frequency disturbances typical for the region.

2. Materials and methods

2.1. Data

We calibrated the CSMatrix-AK model using the largest in situ forest inventory dataset available for the coastal Alaska region with repeated measurements (Peterson et al., 2014). The dataset was derived from the US Pacific-Northwest Forest Inventory Analysis (PNW-FIA) database and contained 544 permanent sample plots (PSPs) for calibration and 244 PSPs for validation (Fig. 1). All selected plots met the following three criteria: (1) at least two measurements were collected from each plot; (2) there was at least one live tree at the time of each measurement; and (3) the plots showed no evidence of substantial silvicultural treatments or human interference.

Over ten species were present in the data, among which western hemlock (*Tsuga heterophylla)* and Sitka spruce (*Picea sitchensis*) constitute 50% of the total stand basal area. For the rest, western red cedar (*Thuja plicata*) and Alaska yellow-cedar (*Cupressus nootkatensis*) were grouped into Alaska cedars; black spruce (*Picea mariana*) and white spruce (*Picea glauca*) were classified together as boreal spruces; and all shade-intolerant trees were categorized into other species (Table 1). Trees were further sorted into nineteen 5-cm diameter-at-breast-height (dbh) classes, with the smallest one consisting of trees ranging from 12.7 to 18 cm in dbh. Only 1% of trees annually grow over 5-cm thus the 5-cm diameter class guarantees that 99% of trees will not move forward by more than one class in annual growth. Negative diameter growth values, generally due to measurement errors and/or shrinkage, accounted for less than 3% of the total population. These negative values were also used to calibrate diameter growth model with the rest of data as the same contribution of measurement errors could be observed on the high-growth end of the diameter growth distribution.

Among the plot-level variables (Table 2), the average recruitment (*R*) was the highest for western hemlock and the lowest for Sitka spruce. The average stand density (*N*) was the highest for western hemlock and the lowest for boreal spruces (Table 3). The average interval between two inventories was ~8 years. At the individual tree level, the Sitka spruce had the largest average diameter at breast height (*D*) and the third largest mortality rate (*m*). Boreal spruces had the smallest average diameter at breast height (*D*) and the second highest average recruitment (*R*) and diameter growth (*g*). Alaska cedars had the lowest average mortality rate (*m*) among all the species (Table 4).

The downscaled 771-m spatial resolution Parameter-Elevation Regression on Independent Slopes Model (PRISM) dataset (http://www.snap.uaf.edu/data.php) was used because it is usually considered more accurate than the WorldClim and Daymet datasets for regional studies (Daly et al., 2008). From the dataset, we extracted the historical climate data from 1995 to 2014 to the temporal and spatial footprint of each plot, based on which we computed mean growing

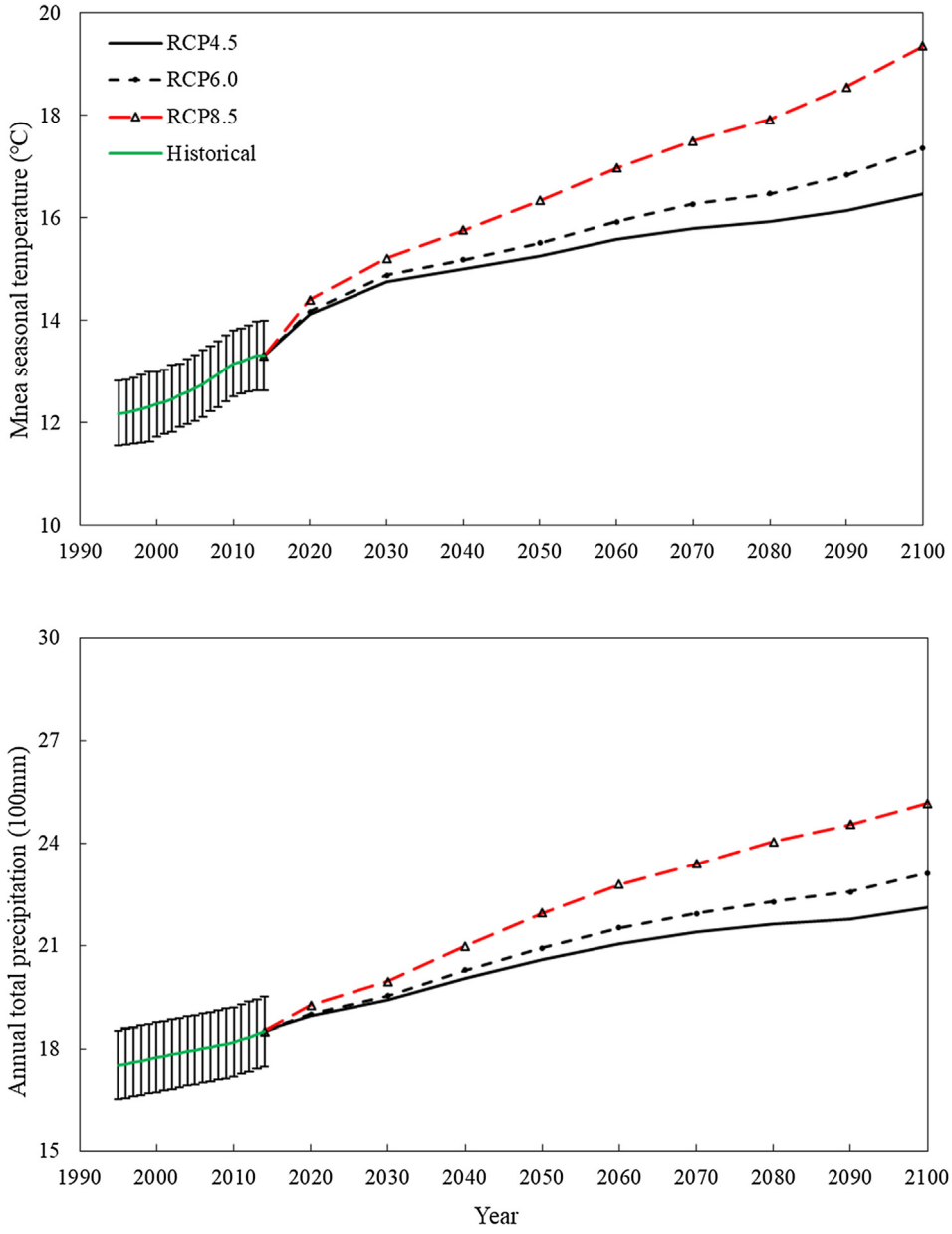

Fig. 2. Historical (mean ± standard deviation) and projected temporal changes of mean growing seasonal temperature (°C) and annual total precipitation (100 mm) across the 244 validation plots under three climate scenarios (i.e. RCP4.5, RCP6.0, and RCP8.5).

seasonal temperatures (*I*, °C) and annual total precipitations (*P*, 100 mm). Spatially explicit future values of *I* and *P* up to Year 2100 were projected using the future trends outlined by the KNMI Climate Change Atlas (http://climexp.knmi.nl/, last accessed 26-August-2018), under three RCP climate scenarios: RCP8.5, RCP6.0, and RCP4.5 (Blyth et al., 2007). RCP8.5 is a business-as-usual scenario with increasing greenhouse gas emissions over time, leading to high greenhouse gas concentration levels; RCP6.0 is a stabilization scenario in which emissions rise quickly until 2060 and then decrease; RCP4.5 assumes quicker actions to limit greenhouse gas emissions with emissions peaking in 2040 and then declining strongly until 2080 (IPCC, 2013).

Across the study region represented by the 244 validation plots (i.e. long-term simulation plots), future mean growing seasonal temperature and annual total precipitation showed an increasing trend under all three RCP scenarios, compared to the climate condition in 2014 (Fig. 2). Mean growing seasonal temperature and annual total precipitation were predicted to have the greatest changes of +6.6 °C under RCP8.5 and +697.2 mm under RCP8.5, respectively, over the next 86 years (2014–2100). RCP4.5 had the smallest increase of temperature and precipitation, +3.7 °C and + 392.0 mm, respectively (Fig. 2).

2.2. Model structure and estimation

A conventional deterministic matrix model (e.g. Buongiorno and Michie, 1980; Picard et al., 2003) predicts the stand-level population dynamics of forest stands from time *t* to *t + 1*:

$$\mathbf{y}_{t+1} = \mathbf{G}\cdot\mathbf{y}_t + \mathbf{R}_t + \varepsilon \quad (1)$$

where $\boldsymbol{y}_t = [y_{ijt}]$ is a column vector representing the number of live trees per ha of species *i* ($i = 1,2,\ldots,m$) and diameter class *j* ($j = 1,2,\ldots,n$) at time *t*. **G** is a state-dependent transition matrix describing the transition of structured population between *t* and *t + 1*. **R** is a regeneration vector and ε is a vector of random errors.

Climate-Sensitive Matrix (CSMatrix) models extend conventional deterministic matrix models by incorporating climate conditions in the transition matrix **G** and regeneration vector **R** (Liang et al., 2011; Ma

Table 5
Estimated parameters of the diameter growth models. Significance levels: * < 0.05; ** < 0.01; *** < 0.001.

	Species											
	WH		MH		SS		AC		BS		OS	
Cons	0.174	***	0.184	***	0.552	***	−0.117		0.022		0.425	***
D	0.002	***	0.00003	*	0.005	***	−0.00003	*	−0.009	*	−0.009	*
D^2	−0.00002	**	−0.00001	*	−0.00003	***	0.00003	*	0.0002	*	0.0001	*
B	−0.001	***	−0.001	***	−0.003	***	−0.001	*	−0.007	***	−0.007	***
C	0.013	***	0.007	***	0.025	***	0.015	***	0.038	***	0.021	***
H_d	−0.060	***	−0.015		−0.111	***	0.041	**	0.107	***	−0.100	***
H_s	−0.029	***	−0.021	**	0.023		−0.039	***	0.009		0.002	
E	0.0001	***	−0.00001		0.0001	*	−0.0001	***	0.00004		−0.0001	*
S	0.0003	***	0.001	***	0.0001		0.001	***	−0.0001		0.001	***
cos(*a*)	0.0001		0.007	**	−0.024	***	0.012	***	0.029	**	0.005	
sin(*a*)	−0.010	***	0.002		−0.003		0.008	*	0.040	***	−0.001	
I	0.00003		0.008		−0.055	***	0.024		−0.041		−0.007	***
P	0.001		−0.004	***	−0.007	*	0.003		0.022		−0.008	
I·P	−0.0002	*	−0.0004	**	0.0003		−0.00003		0.007		0.0002	
I^2	0.0003		−0.001		0.004	*	−0.001		0.012	***	−0.001	
P^2	0.00002		0.0001	***	0.0001	*	0.0001		−0.001		0.0001	*
R^2	0.79		0.76		0.71		0.68		0.70		0.66	
AIC	7452		8261		9856		10,264		8856		11,632	
BIC	7569		8364		9913		10,326		8951		11,812	

Table 6
Estimated parameters of the mortality models. Significance levels: * < 0.05; ** < 0.01; *** < 0.001.

	Species											
	WH		MH		SS		AC		BS		OS	
Cons	−1.130	*	−2.712	***	−1.020		−0.398		−5.157		−2.314	***
D	−0.009	**	0.006	*	−0.015	**	−0.013	**	0.181	**	0.017	*
D^2	0.0001		−0.0001	*	0.0001	**	0.0001		−0.003	*	−0.0004	*
B	0.002	*	−0.007	*	0.004		0.005	*	0.020	*	0.012	*
C	−0.024		0.011		0.025	*	0.044	*	0.003		−0.021	*
H_d	−0.052	*	−0.218		0.238	*	−0.312	*	−0.669	*	0.351	*
H_s	−0.024	*	0.370	*	0.354	*	0.089		0.725		−0.160	*
E	−0.0004		0.0001		−0.002	*	0.001		0.001	*	−0.0001	
S	0.002		0.004		0.003		−0.005		−0.020	***	−0.003	
cos(*a*)	−0.022		−0.003		−0.031		−0.019		−0.206		0.042	
sin(*a*)	0.028		−0.042		0.006		0.002		0.069		0.135	
I	0.039	**	0.162		0.135	*	−0.037		−0.117	**	0.108	*
P	−0.018	*	0.033		0.045		−0.012		−0.454	*	−0.009	*
I·P	0.003	*	−0.010	***	−0.003		0.013	*	0.133	*	0.004	*
I^2	−0.009	*	0.019		−0.0002		−0.027		0.116		−0.022	*
P^2	−0.0001	*	0.0003		0.0002		−0.002		−0.053	*	−0.0002	
R^2	0.28		0.23		0.22		0.19		0.25		0.26	
AIC	4152		4526		4626		4896		4362		4295	
BIC	4231		4612		4698		4985		4421		4320	

et al., 2016; Ma and Zhou, 2017):

$$\mathbf{y}_{t+1} = \mathbf{G}(T, P)\cdot\mathbf{y}_t + \mathbf{R}(T, P) + \varepsilon \quad (2)$$

Stochastic CSMatrix-AK model is developed from the deterministic CSMatrix-AK model (Eq. (2)) by replacing the random error vector ε with a vector of stochastic shocks, u_{t+1}:

$$y_{t+1} = \mathbf{G}_t(T, P)\cdot y_t + \mathbf{R}_t(T, P) + u_{t+1} \quad (3)$$

where u_{t+1} is generated by bootstrapping from the set of annualized differences between the predictions by the deterministic CSMatrix-AK model and the observed values.

$\mathbf{G}_t$ and $\mathbf{G}_{it}$ are matrices used to model forest population dynamics at time *t*, where:

$$\mathbf{G}_t = \begin{bmatrix} \mathbf{G}_{1_t} & & & \\ & \mathbf{G}_{2_t} & & \\ & & \ddots & \\ & & & \mathbf{G}_{m,t} \end{bmatrix}$$

$$\mathbf{G}_{it} = \begin{bmatrix} a_{i1,t} & & & & \\ b_{i1,t} & a_{i2,t} & & & \\ & \ddots & \ddots & & \\ & & b_{i,n-2,t} & a_{i,n-1,t} & \\ & & & b_{i,n-1,t} & a_{i,n,t} \end{bmatrix} \quad (4)$$

in which a_{ijt} represents the probability that a tree of species *i* and diameter class *j* stays alive in the same diameter class between *t* and *t + 1*. b_{ijt}, the probability of upgrowth, is estimated as the tree diameter growth g_{ijt} between *t* and *t + 1* divided by the width of the diameter class, assuming that trees are evenly distributed within a diameter class. a_{ijt} and b_{ijt} are related by:

$$a_{ijt} = 1 - b_{ijt} - m_{ijt} \quad (5)$$

where m_{ijt} is the probability of tree mortality between *t* and *t + 1*.

$\mathbf{R_t}$ is a state-, time-, and climate-dependent recruitment vector representing the number of trees naturally recruited in the smallest diameter class of each species, between *t* and *t + 1*:

Table 7
Estimated parameters of the recruitment models. Significance levels: * < 0.05; ** < 0.01; *** < 0.001.

	Species											
	WH		MH		SS		AC		BS		OS	
Cons	−19.141	***	−13.150	***	−20.863	**	−13.682		−5.171		−6.108	
N	0.030	***	0.017	***	0.047	***	0.031	*	0.091	***	0.068	**
N^2	−0.015	**	−0.004		−0.020	*	−0.029	*	−0.116	***	−0.001	*
B	−0.046	*	−0.024		−0.113	*	−0.035		−0.248	*	−0.214	*
C	0.309	*	−0.708	*	0.423		−0.008		0.796		0.512	
H_d	−2.357	*	0.858	*	−6.075	**	−1.475	*	0.146		−5.513	*
H_s	1.123		2.254	*	−0.092		3.295	**	−1.766	*	6.600	*
E	−0.001		0.007	**	−0.003		−0.001		0.011		−0.013	
S	−0.001		0.030		0.076	*	0.021		0.094	*	−0.007	
cos(*a*)	−0.535		0.476		−0.830		0.054		1.072		−1.976	
sin(*a*)	−0.099		0.322		1.708		0.281		−0.063		−0.901	
I	2.945	*	0.579		−3.448		1.427	**	0.732		−2.810	
P	0.395		0.264		−0.963	**	0.045	*	−1.705		0.266	
I·P	−0.048	*	−0.036		0.043		−0.018	*	0.117		0.102	
I^2	−0.067		0.029		0.227		−0.017	*	−0.356		0.016	
P^2	−0.0005		−0.002		−0.015	*	0.002	*	−0.030		−0.010	
R^2	0.36		0.33		0.30		0.29		0.35		0.31	
AIC	5321		5562		5748		5863		5456		5695	
BIC	5429		5633		5799		5924		5510		5716	

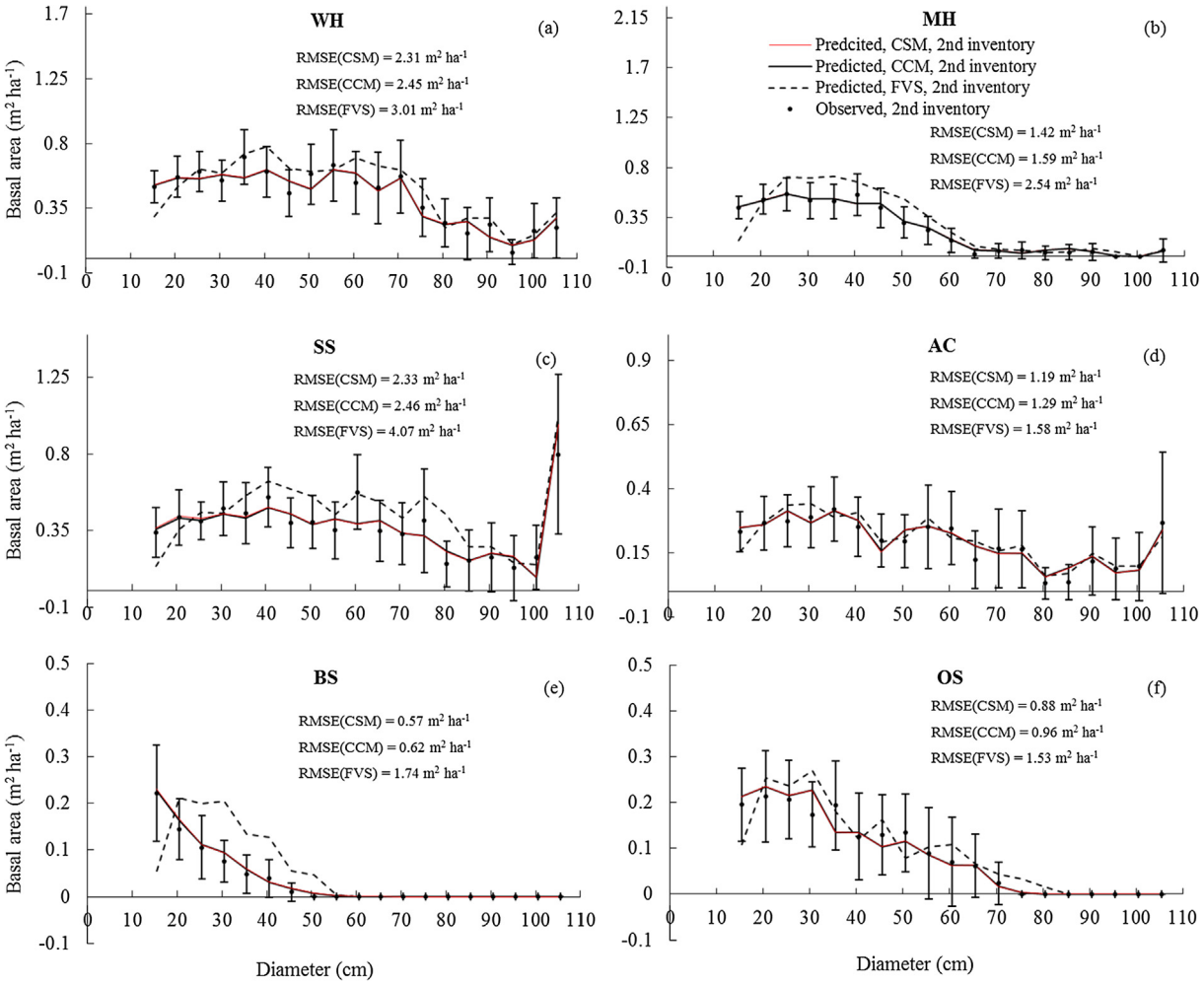

Fig. 3. Average observed and predicted stand basal area at the second inventory from climate-sensitive matrix model (CSM), climate-constant matrix model (CCM), and FVS on the 244 post-sample validation plots, with 95% confidence interval of the observed mean values.

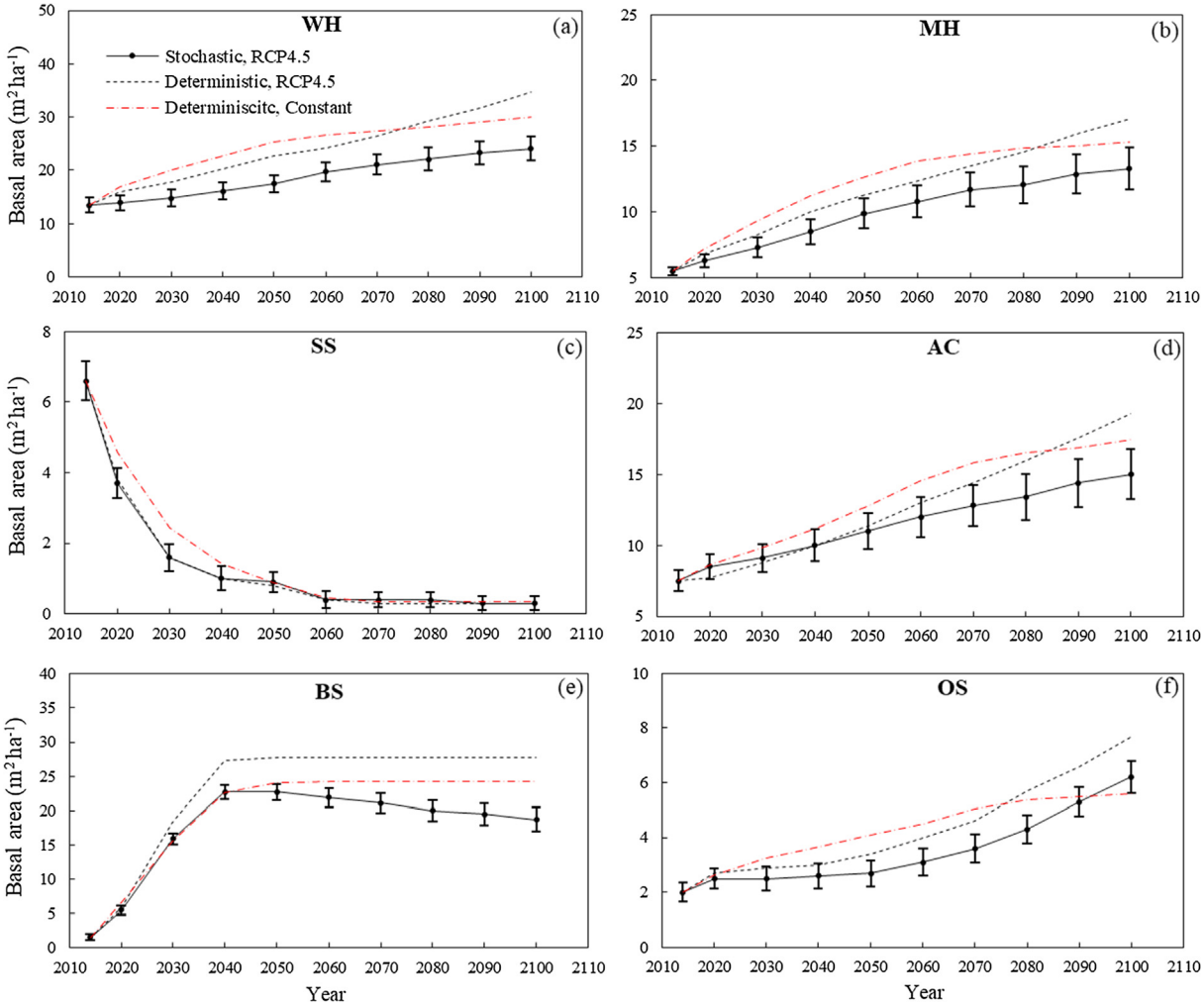

Fig. 4. Deterministic and stochastic predictions of stand basal area ($m^2\ ha^{-1}$) of six species groups from 2014 to 2100 under constant climate and climate scenario RCP4.5.

$$\mathbf{R}_t = \begin{bmatrix} \mathbf{R}_{1t} \\ \mathbf{R}_{2t} \\ \vdots \\ \mathbf{R}_{m,t} \end{bmatrix}, \mathbf{R}_{it} = \begin{bmatrix} R_{it} \\ 0 \\ \vdots \\ 0 \end{bmatrix} \quad (6)$$

We adopted the same variables and functional form for the underlying diameter growth, mortality, and recruitment equations as those established in the published matrix growth models (e.g., Liang et al., 2011; Liang and Zhou, 2014; Ma et al., 2016; Ma and Zhou, 2017) to avoid overfitting and multicollinearity issues. A variety of tree and stand level variables selected for six species groups were used in the matrix growth models (Table 2). Diameter and its square (D, D^2) were applied in the individual tree models (diameter growth, mortality) to account for the nonlinear influences of diameter on growth (e.g., Liang et al., 2005; Ma et al., 2018a). The stand density of that species and its square (N, N^2), representing the size of seed bank (Peterson et al., 2014), were only used in the stand-level recruitment model. Many existing matrix models use total stand basal area (B) and site productivity (C) as key predictors, due to their significant effects on forest dynamics (Namaalwa et al., 2005; Boltz and Carter, 2006; Ma et al., 2018b). Physiographic variables, such as elevation (E), slope (S), and aspect (a), were used to control for site productivity (Lennon et al., 2002). In addition, stand diversity metrics of structural and species diversity (H_d, H_s) were included to explicitly explain the impacts of diversity on forest dynamics (i.e. positive relationship between plant diversity and net ecosystem productivity; Liang et al., 2007). Climatic variables (I, P) were added to explore the effects of temperature and precipitation on diameter growth, mortality, and recruitment (Liang et al., 2011).

The diameter growth of the tree of species i and size class j from t and $t + 1$ considering climate change was represented by the following model (Liang et al., 2011; all notations defined in Table 2):

$$g_{ij} = \alpha_{i1} + \alpha_{i2}D + \alpha_{i3}D^2 + \alpha_{i4}B + \alpha_{i5}C + \alpha_{i6}H_d + \alpha_{i7}H_s + \alpha_{i8}E + \alpha_{i9}S + \alpha_{i10}\cos(a) + \alpha_{i11}\sin(a) + \alpha_{i12}I + \alpha_{i13}P + \alpha_{i14}I{\cdot}P + \alpha_{i15}I^2 + \alpha_{i16}P^2 + \beta_{ij} \quad (7)$$

in which α_{ij} are parameters to be estimated with the ordinary least squares for diameter growth of species i and diameter class j. g_{ij} was then calculated with Eq. (7) in which D was replaced by the midpoint of each diameter class D_j.

Tree mortality, m_{ij}, was estimated with a Probit function (Ai and Norton, 2003):

$$m_{ij} = \Phi(\delta_{i1} + \delta_{i2}D + \delta_{i3}D^2 + \delta_{i4}B + \delta_{i5}C + \delta_{i6}H_d + \delta_{i7}H_s + \delta_{i8}E + \delta_{i9}S + \delta_{i10}\cos(a) + \delta_{i11}\sin(a) + \delta_{i12}I + \delta_{i13}P + \delta_{i14}I{\cdot}P + \delta_{i15}I^2 + \delta_{i16}P^2) + \xi_{ij} \quad (8)$$

where Φ is the standard normal cumulative function, δ_{ij} are parameters estimated by the maximum likelihood.

Recruitment of species i, R_i, was estimated with a Tobit model

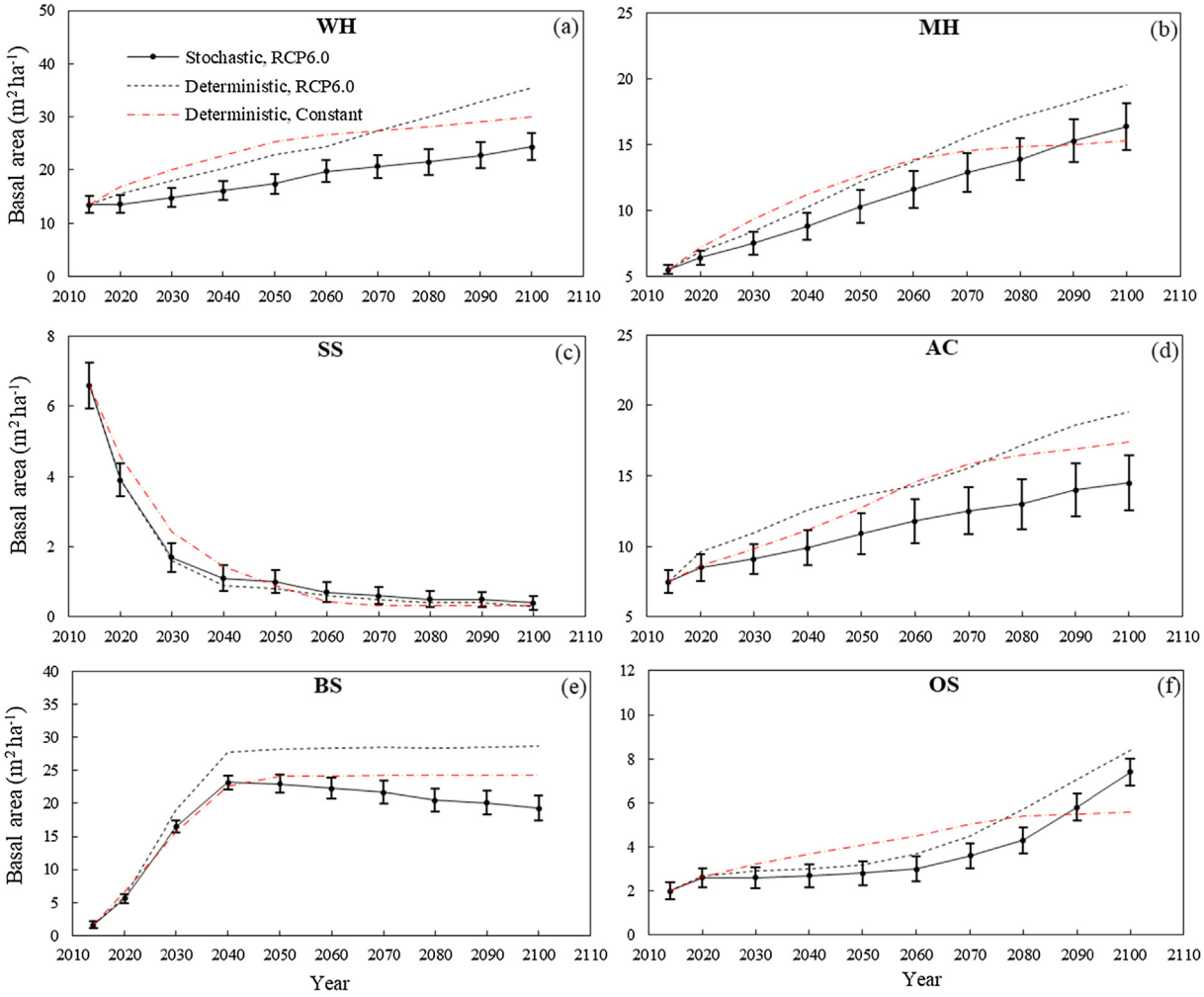

Fig. 5. Deterministic and stochastic predictions of basal area (m^2 ha^{-1}) of six species groups from 2014 to 2100 under constant climate and climate scenario RCP6.0.

(Tobin, 1958) to account for left-censored recruitment values at the preset diameter limit:

$$R_{it} = \Phi(\beta_i x_{it} \sigma_i^{-1})\beta_i x_{it} + \sigma_i \phi(\beta_i x_{it} \sigma_i^{-1}) \quad (9)$$

with

$$\beta_i x_{it} = \beta_{i1} + \beta_{i2}N + \beta_{i3}N^2 + \beta_{i4}B + \beta_{i5}C + \beta_{i6}H_d + \beta_{i7}H_s + \beta_{i8}E + \beta_{i9} S + \beta_{i10}\cos(a) + \beta_{i11}\sin(a) + \beta_{i12}I + \beta_{i13}P + \beta_{i14}I{\cdot}P + \beta_{i15} I^2 + \beta_{i16}P^2 + \mu_{ij} \quad (10)$$

where Φ is the standard normal cumulative distribution function and φ is the standard normal probability density function.

Both tree species diversity (H_s) and tree size diversity (H_d) were represented by Shannon's entropy measure (Pielou, 1977):

$$H_s = -\sum_{i=1}^{m} \frac{B_i}{B} \ln\left(\frac{B_i}{B}\right), \quad H_d = -\sum_{j=1}^{n} \frac{B_j}{B} \ln\left(\frac{B_j}{B}\right) \quad (11)$$

where B_i, B_j and B were, respectively, the basal area of species i, diameter class j and total stand basal area.

The stochastic simulations were implemented by adding stochastic shocks to all sample plots at each 1-year time step. We used a bootstrapping approach (Runkle, 1987; Diebold et al., 1998; Liang et al., 2006) to derive the stochastic shock vectors u_{t+1}, by drawing randomly with replacement from a sample of 544 independent annualized differences between predictions by the deterministic CSMatrix-AK model and observations. We performed 100,000 bootstrap iterations to derive the mean and standard errors of the predicted values. This approach only accounted for the effects of small-scale and high-frequency disturbances typical for the region, such as spruce-beetle outbreaks, windthrow, avalanches, and landslides throughout coastal Alaska region (Lertzman et al., 1996; Kramer et al., 2001; Kirkland and Barrett, 2016), on stand growth, owing to the short intervals between two consecutive inventories (~8 years), even though the sample plots extended across a vast 2.4 million-ha region. Nevertheless, such disturbances play an important role in forest composition and population dynamics (Bjørnstad and Grenfell, 2001; Zhou and Buongiorno, 2004).

3. Results

3.1. Model parameters and validation

Tables 5–7 summarize the estimated parameters of the matrix growth models. The effects of non-climatic variables on diameter growth, mortality, and recruitment were in general significant and consistent with previous findings. Climatic variables were significant for diameter growth of mountain hemlock and Sitka spruce, mortality of western hemlock and boreal spruces, and recruitment of Alaska cedars.

For the 244 post-sample validation plots, the basal area by diameter class and species group predicted by the CSMatrix-AK model all fell within the 95% confidence intervals of the observed mean values (Fig. 3). The CSMatrix-AK model (RMSE = 8.70 m^2 ha^{-1}) reduced the RMSE by 7.15% from the CCMatrix model (RMSE = 9.37 m^2 ha^{-1}). In

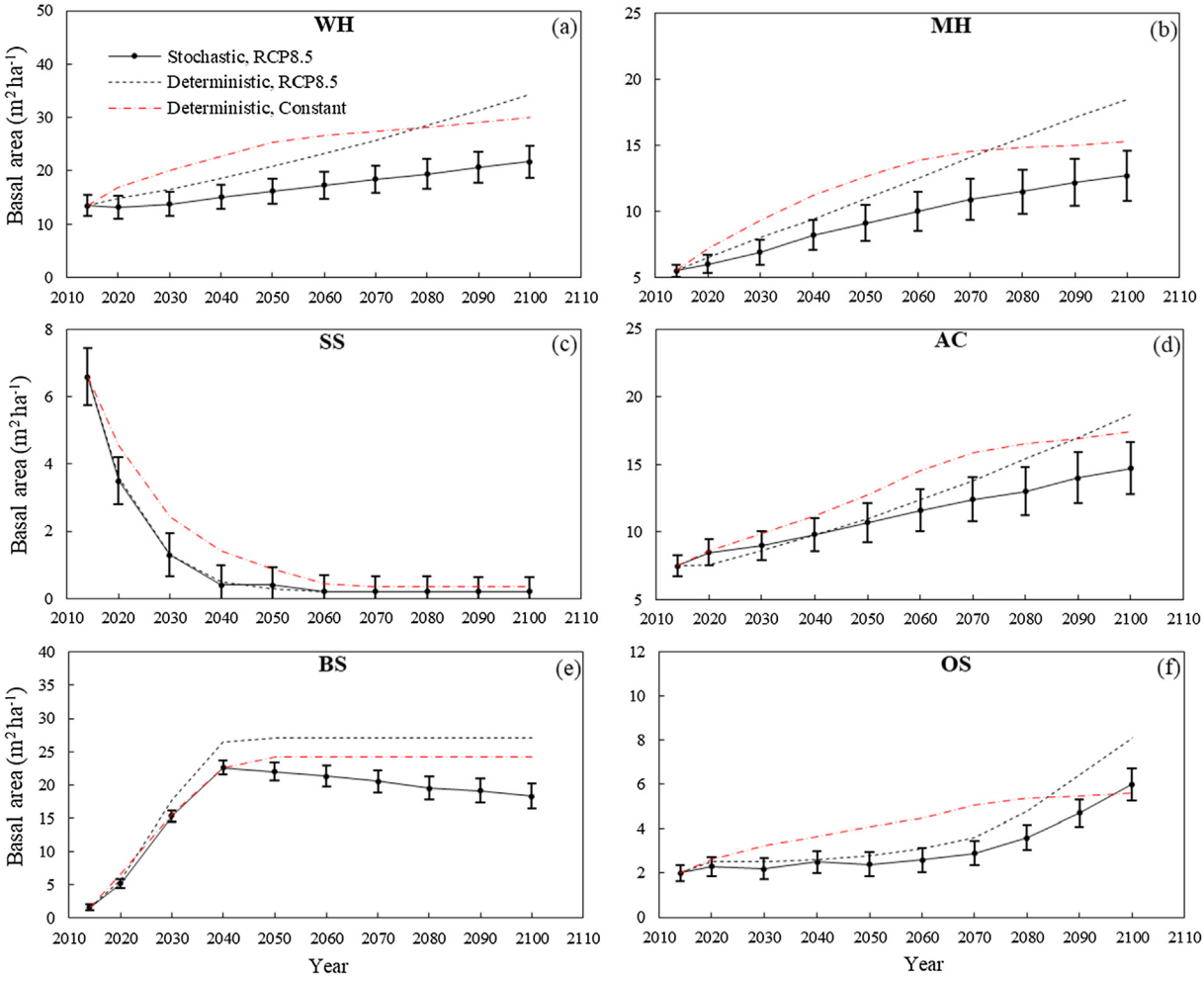

Fig. 6. Deterministic and stochastic predictions of basal area ($m^2\ ha^{-1}$) of six species groups from 2014 to 2100 under constant climate and climate scenario RCP8.5.

comparison, predictions of FVS largely fell outside the 95% confidence intervals of the observed mean values. FVS underestimated the basal area of the smallest trees, and systematically overestimated the basal area of trees larger than 20 cm in diameter (Fig. 3). Thus, CSMatrix-AK was in general more accurate than the CCMatrix model and the FVS for all species groups.

3.2. Future projection under constant climate

Under a constant climate, the predicted basal area of western hemlock, mountain hemlock, Alaska cedars, boreal spruces, and other species increased at the beginning and then converged to ~30.0, ~15.3, ~17.4, ~24.2, and ~5.6 $m^2\ ha^{-1}$, respectively (Fig. 4). However, the predicted basal area of Sitka spruce decreased to nearly zero from the year 2014 to 2100 (Fig. 4). The total basal area increased over the first 60 years and converged to ~92.8 $m^2\ ha^{-1}$.

3.3. Future projections under climate change without disturbances

Compared to a constant climate without considering disturbances, climate change decreased the basal area of western hemlock, mountain hemlock, Alaska cedars, and other species over the first 50 years, but then significantly increased it at the end of 2100 under the three climate scenarios (Figs. 4–6). Sitka spruce would have similar basal area under the three IPCC scenarios in year 2100 (Figs. 4c, 5c, and 6c). Climate change would increase the basal area of boreal spruces from 2025 to 2100 (Fig. 4e, 5e, and 6e). Total stand basal area would increase over time but no convergent values would be reached by the year 2100 (Table 8 and Fig. 7).

3.4. Future projections under climate change with disturbances

Considering stochastic shocks under climate change, based on 100,000 simulations, the basal area of each species and the total stand basal area accompanying with confidence intervals would be smaller in general than deterministic predictions (Figs. 4–7). Total stand basal area under the three RCP scenarios (i.e. RCP4.5, RCP6.0, and RCP8.5) increased over the next 80 years and converged to the range of 73.6–82.4 $m^2\ ha^{-1}$ (Table 9 and Fig. 7). In terms of species composition as percentage of basal area, current forests in the coastal Alaska are dominated by western hemlock and Sitka spruce. While considering disturbances under climate change, forests in the coastal Alaska in year 2100 would be dominated by western hemlock and boreal spruces.

4. Discussion and conclusion

Tested on 244 validation plots, basal area predictions of the CSMatrix-AK model all fell within the 95% confidence intervals of the observed mean values. In contrast, FVS projects recruitment and regeneration if and only if the stand density is below a predesignated threshold value (Dixon et al., 1992; Crookston et al., 2010) and is shown to systematically undermine the accuracy of the entire model, even for short-term predictions. In comparison to the CCMatrix model which ignores climatic impacts on diameter growth, mortality, and recruitment, our CSMatrix-AK model also displayed greater accuracy because these impacts are found to be more substantial in Alaska than

Table 8
Deterministic predictions of basal area (m^2 ha^{-1}) from 2014 to 2100 under constant climate and three climate scenarios (i.e. RCP4.5, RCP6.0, and RCP8.5).

Species	2014	2020	2030	2040	2050	2060	2070	2080	2090	2100
	Constant Climate									
WH	13.5	16.8	20.0	22.6	25.4	26.7	27.3	28.1	29.0	29.9
MH	5.5	7.2	9.3	11.2	12.7	13.9	14.4	14.9	15.0	15.3
SS	6.6	4.6	2.4	1.4	0.9	0.4	0.3	0.3	0.3	0.3
AC	7.5	8.6	9.9	11.2	12.8	14.6	15.8	16.5	16.9	17.4
BS	1.6	6.6	15.6	22.6	24.1	24.2	24.2	24.3	24.3	24.3
OS	2.0	2.6	3.2	3.7	4.1	4.5	5.1	5.4	5.5	5.6
Total	36.7	46.4	60.5	72.7	78.0	84.2	87.2	89.5	91.0	92.8
	RCP4.5									
WH	13.5	15.9	17.9	20.2	22.7	24.2	26.4	29.3	31.8	34.8
MH	5.5	6.8	8.3	10.0	11.3	12.4	13.5	14.6	15.9	17.1
SS	6.6	3.8	1.6	1.0	0.8	0.4	0.3	0.3	0.3	0.2
AC	7.5	7.7	8.8	10.2	11.4	13.0	14.4	16.0	17.6	19.3
BS	1.6	5.9	18.4	27.3	27.8	27.8	27.9	27.9	28.0	28.1
OS	2.0	2.7	2.9	3.0	3.4	4.0	4.6	5.7	6.6	7.7
Total	36.7	42.8	57.9	71.5	77.4	81.8	87.0	93.7	100.2	107.1
	RCP6.0									
WH	13.5	15.6	18.0	20.3	22.9	24.4	27.4	30.1	32.8	35.5
MH	5.5	6.9	8.4	10.2	12.2	13.7	15.6	17.1	18.3	19.6
SS	6.6	3.9	1.6	0.9	0.8	0.6	0.5	0.4	0.4	0.3
AC	7.5	9.6	11.0	12.6	13.6	14.3	15.6	17.2	18.6	19.5
BS	1.6	5.9	19.0	27.8	28.2	28.4	28.5	28.5	28.5	28.6
OS	2.0	2.7	2.9	3.0	3.2	3.7	4.5	5.7	7.1	8.4
Total	36.7	44.6	60.9	74.8	80.9	85.1	92.1	98.9	105.7	111.9
	RCP8.5									
WH	13.5	14.9	16.6	18.6	20.8	23.2	25.8	28.5	31.4	34.4
MH	5.5	6.5	8.0	9.4	11.0	12.5	14.1	15.6	17.1	18.5
SS	6.6	3.6	1.3	0.5	0.3	0.2	0.2	0.2	0.2	0.2
AC	7.5	7.6	8.6	9.8	11.1	12.4	13.8	15.4	17.0	18.7
BS	1.6	5.7	17.7	26.5	27.0	27.1	27.1	27.2	27.2	27.3
OS	2.0	2.5	2.5	2.6	2.8	3.1	3.6	4.8	6.4	8.1
Total	36.7	40.8	54.7	67.4	72.9	78.4	84.5	91.5	99.1	106.9

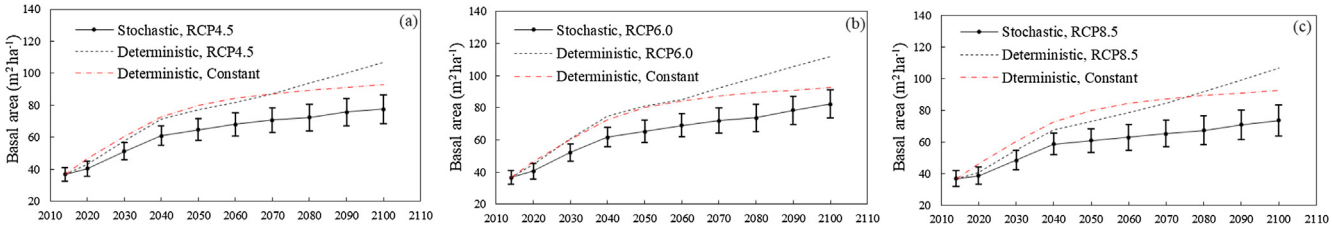

Fig. 7. Deterministic and stochastic predictions of total stand basal area (m^2 ha^{-1}) from 2014 to 2100 under constant climate and three climate scenarios (i.e. RCP4.5, RCP6.0, and RCP8.5).

in most other regions worldwide (Juday et al., 1998; Serreze et al., 2000).

Our CSMatrix-AK model shows that climatic factors including temperature and precipitation significantly affected diameter growth of mountain hemlock and Sitka spruce, mortality of western hemlock, Sitka spruce, and boreal spruces, and recruitment of western hemlock, Sitka spruce, and Alaska cedars. Consequently, boreal spruces (including white spruce and black spruce) would become much more common by 2040, as boreal spruces had higher recruitment and growth rate. The dramatic decline of Sitka spruce was attributable to the species' lower recruitment and higher mortality driven by an increasing mean growing seasonal temperature. These results support that climate change has a profound impact on diameter growth, mortality, and recruitment for different species, which in turn affects forest dynamics at high latitudes (Zhang et al., 2015).

Some studies predict that climate change will accelerate forest growth (Boisvenue and Running, 2006; Pretzsch et al., 2014), but it is important to note that diameter growth, mortality, and recruitment are three essential components of forest dynamics that can be affected considerably by natural disturbances (Fischer et al., 2013). Concern is mounting for high-latitude regions with increasing natural disturbances under climate change (Dale et al., 2001). When disturbances were accounted for in this study, we projected a reduced total stand basal area under three climate scenarios, consistent with the finding in Bergeron (2000). It suggests, in the high latitude regions such as coastal Alaska, warmer climate would increase water availability in snow-dominated regions (Barnett et al., 2005), but disturbances can more than offset this positive effect of climate change, leading to a forest stock lower than the expected level. Although our study only considered small-scale, high-frequency stochastic events, even these small shocks could aggregate to exert considerable impacts on coastal Alaska forests.

The stochastic CSMatrix-AK model enables stand-level estimates of structured forest dynamics under climate change, useful for small-scale forest management and silvicultural studies. This type of model can be applied to evaluating management and harvesting regimes of timber and carbon (Liang, 2010; Ma and Zhou, 2017), assessing impacts of fire regimes under future climate change (Rupp, 2008; Ma et al., 2016), and quantifying tradeoffs between different economic and ecological objectives (Zhou et al., 2008; Ma and Zhou, 2017). Additionally, the capability of predicting species- and size-specific forest population dynamics over time with high accuracy also makes the CSMatrix-AK model a good benchmark for future development of empirical and

Table 9
Stochastic predictions (± standard deviation) of basal area (m^2 ha^{-1}) from 2020 to 2100 under constant climate and three climate scenarios (i.e. RCP4.5, RCP6.0, and RCP8.5).

Species	2020	2030	2040	2050	2060	2070	2080	2090	2100
					RCP4.5				
WH	13.9 ± 1.5	14.8 ± 1.5	16.1 ± 1.6	17.5 ± 1.6	19.8 ± 1.8	21.1 ± 1.9	22.1 ± 2.1	23.3 ± 2.2	24.1 ± 2.3
MH	6.3 ± 0.5	7.3 ± 0.8	8.5 ± 0.9	9.9 ± 1.1	10.8 ± 1.2	11.7 ± 1.3	12.1 ± 1.4	12.9 ± 1.5	13.3 ± 1.6
SS	3.7 ± 0.4	1.6 ± 0.4	1.0 ± 0.3	0.9 ± 0.3	0.4 ± 0.2	0.4 ± 0.2	0.4 ± 0.2	0.3 ± 0.1	0.3 ± 0.1
AC	8.5 ± 0.9	9.1 ± 1.0	10.0 ± 1.1	11.1 ± 1.3	12.2 ± 1.4	12.8 ± 1.5	13.4 ± 1.6	14.4 ± 1.7	15.0 ± 1.7
BS	5.5 ± 0.6	15.9 ± 0.8	22.7 ± 1.0	22.5 ± 1.2	21.9 ± 1.4	21.1 ± 1.5	20.0 ± 1.6	19.5 ± 1.6	18.7 ± 1.7
OS	2.5 ± 0.4	2.5 ± 0.4	2.6 ± 0.5	2.7 ± 0.5	3.1 ± 0.5	3.6 ± 0.5	4.3 ± 0.5	5.3 ± 0.5	6.2 ± 0.6
Total	40.4 ± 4.3	51.2 ± 4.9	60.9 ± 5.4	64.7 ± 6.0	68.0 ± 6.6	70.7 ± 6.9	72.3 ± 7.4	75.7 ± 7.7	77.6 ± 8.1
					RCP6.0				
WH	13.6 ± 1.7	14.8 ± 1.7	16.1 ± 1.8	17.4 ± 1.8	19.8 ± 2.0	20.7 ± 2.1	21.5 ± 2.4	22.8 ± 2.4	24.4 ± 2.5
MH	6.4 ± 0.5	7.5 ± 0.9	8.8 ± 1.0	10.3 ± 1.3	11.6 ± 1.4	12.9 ± 1.5	13.9 ± 1.6	15.3 ± 1.7	16.4 ± 1.8
SS	3.9 ± 0.5	1.7 ± 0.4	1.1 ± 0.4	1.0 ± 0.3	0.7 ± 0.3	0.6 ± 0.2	0.5 ± 0.2	0.5 ± 0.1	0.4 ± 0.1
AC	8.5 ± 1.0	9.1 ± 1.1	9.9 ± 1.2	10.9 ± 1.5	11.8 ± 1.5	12.5 ± 1.7	13.0 ± 1.8	14.1 ± 1.9	14.5 ± 2.0
BS	5.6 ± 0.7	16.5 ± 0.9	23.2 ± 1.1	23.0 ± 1.4	22.3 ± 1.6	21.7 ± 1.7	20.5 ± 1.8	20.1 ± 1.8	19.3 ± 1.9
OS	2.6 ± 0.4	2.6 ± 0.5	2.7 ± 0.5	2.8 ± 0.5	3.0 ± 0.6	3.6 ± 0.6	4.3 ± 0.6	5.8 ± 0.6	7.4 ± 0.6
Total	40.6 ± 4.8	52.2 ± 5.4	61.8 ± 6.0	65.4 ± 6.8	69.2 ± 7.4	72.0 ± 7.8	73.7 ± 8.3	78.5 ± 8.6	82.4 ± 9.0
					RCP8.5				
WH	13.2 ± 2.2	13.8 ± 2.2	15.1 ± 2.3	16.2 ± 2.3	17.3 ± 2.5	18.4 ± 2.6	19.4 ± 2.9	20.7 ± 2.9	21.7 ± 3.0
MH	6.0 ± 0.7	6.9 ± 1.0	8.2 ± 1.1	9.1 ± 1.4	10.0 ± 1.5	10.9 ± 1.6	11.5 ± 1.7	12.2 ± 1.8	12.7 ± 1.9
SS	3.5 ± 0.7	1.3 ± 0.6	0.4 ± 0.5	0.4 ± 0.4	0.2 ± 0.3	0.2 ± 0.2	0.2 ± 0.2	0.2 ± 0.1	0.2 ± 0.1
AC	8.5 ± 1.0	9.0 ± 1.1	9.8 ± 1.2	10.7 ± 1.4	11.6 ± 1.6	12.4 ± 1.6	13.0 ± 1.8	14.1 ± 1.9	14.7 ± 1.9
BS	5.2 ± 0.7	15.3 ± 0.9	22.6 ± 1.1	22.0 ± 1.4	21.3 ± 1.6	20.5 ± 1.7	19.5 ± 1.7	19.1 ± 1.8	18.3 ± 1.8
OS	2.3 ± 0.4	2.2 ± 0.5	2.5 ± 0.5	2.4 ± 0.5	2.6 ± 0.6	2.9 ± 0.6	3.6 ± 0.6	4.7 ± 0.7	6.0 ± 0.7
Total	38.7 ± 5.6	48.5 ± 6.3	58.6 ± 6.8	60.8 ± 7.5	63.0 ± 8.2	65.3 ± 8.5	67.2 ± 9.1	70.9 ± 9.4	73.6 ± 9.9

process-based growth models for the region. Like most empirical models, our stochastic CSMatrix-AK model has its limitations. As its geographic coverage was limited to coastal Alaska, caution is advised when applying this model outside of the study area. In addition, any long-term projection results should be interpreted with caution, especially when the future climate conditions go beyond current observed range. Nevertheless, our stochastic CSMatrix-AK model offered a compelling illustration of forest dynamics subject to climate change and small-scale, high-frequency shocks and provided a valuable tool for forest researchers and managers to understand future forest growth. In addition, the unprecedented accuracy of the model made it a useful tool for assessing forest carbon dynamics and associated ecological and climatic implications, quantifying forest management outcomes, and optimizing for economic or ecological objectives.

As shown in the literature, climate change would have significant impacts on forest species composition by affecting the distribution and variation of key environmental factors, such as humidity and incoming solar radiation (e.g., Aber et al., 2001; Latta et al., 2010; Schoene and Bernier, 2012), as well as forest ecosystem processes through alterations in resource acquisition and utilization efficiency (Hansen et al., 2001; Juday et al., 2005). Our results provided more empirical evidences supporting these findings and showed that a warmer and more variable climate was expected to substantially alter the diameter growth, establishment, and distribution of Sitka spruce and boreal spruce, consistent with previous findings (Abrahamson, 2015; Mason and Perks, 2011). Intolerant to warmer climate and drought-stress, Sitka spruce was projected to decline as climate change brings warmer and drier conditions which may increase the susceptibility of this species to pests and diseases (Desprez-Loustau et al., 2006). Such changes would cause higher mortality and lower growth and establishment of Sitka spruce, which in turn could diminish Sitka spruce in the future warmer condition across the coastal Alaska region. On the other hand, our and prior studies (Abrahamson, 2015; Stokes et al., 2018) suggest that white spruce may have increased growth rates and increased stand density as a result of decreased mortality under a warmer climate, supported by the ongoing trend that white spruce is becoming widespread and increasingly dominant throughout Alaska and all of the western Canadian provinces (Dyrness, 1980).

Our projected replacement of Sitka spruce by boreal spruce species under climate change across the coastal Alaska region has profound ecological and economic implications. Such a fundamental shift in dominant tree species will change habitat structure, i.e. canopy light, temperature, moisture, litter, and decaying wood, and key ecosystem processes, such as soil nutrient cycling, throughfall and interception loss, and litter inputs and chemistry (Ford and Deans, 1978; Ma et al., 2016). More importantly, a decline of Sitka spruce will have a detrimental effect on the forest industry in the region which is heavily dependent on timber from this species. In light of this discovery, we recommend that forest managers and landowners start searching for substitute species for sawlogs or fiber products (Macdonald and Hubert, 2002), and adapting their management strategies with alternate harvesting plans, rotation lengths, etc., to future scarcity of Sitka spruce. Furthermore, the predicted reduction of total basal area may, to a certain degree, further impair the forest sector in the region. Local communities would need to be better informed and prepared for such socioeconomic impacts of climate change.

Acknowledgements

This research was funded in part by a Joint Venture Agreement between Forest Service Pacific Northwest Research Station and West Virginia University (15-JV-11261975-070), and by the Department of Forestry and Natural Resources, Purdue University. We thank Dr. Eungul Lee for his assistance with the climate data and comments on an early draft. The usual disclaimer applies.

Appendix A. Supplementary material

Supplementary data to this article can be found online at https://doi.org/10.1016/j.foreco.2019.06.030.

References

Ai, C., Norton, E.C., 2003. Interaction terms in logit and probit models. Econ. Lett. 80, 123–129.
Aber, J., Neilson, R.P., Mcnulty, S., Lenihan, J.M., Bachelet, D., Drapek, R.J., 2001. Forest processes and global environmental change: predicting the effects of individual and

multiple stressors. Bioscience 51, 735–751.
Abrahamson, Ilana, 2015. Picea glauca, white spruce. In: Fire Effects Information System, [Online]. U.S. Department of Agriculture, Forest Service, Rocky Mountain Research Station, Fire Sciences Laboratory (Producer). Available: https://www.fs.fed.us/database/feis/plants/tree/picgla/all.html.
Berman, M., Juday, G.P., Burnside, R., 1998. Climate change and Alaska's forests: people, problems, and policies. In: Implications of Global Change in Alaska and the Bering Sea Region. Proceedings of a workshop at the University of Alaska Fairbanks, pp. 29–30.
Barnes, G.H., 1962. Yield of even-aged stands of western hemlock (No. 1273). US Dept of Agriculture.
Blyth, W., Yang, M., Bradley, R., 2007. Climate Policy Uncertainty and Investment Risk. OECD Publishing.
Buongiorno, J., Michie, B.R., 1980. A matrix model of uneven-aged forest management. For. Sci. 26, 609–625.
Boltz, F., Carter, D.R., 2006. Multinomial logit estimation of a matrix growth model for tropical dry forests of eastern Bolivia. Can. J. For. Res. 36, 2623–2632.
Bjørnstad, O.N., Grenfell, B.T., 2001. Noisy clockwork: time series analysis of population fluctuations in animals. Science 293, 638–643.
Boisvenue, C., Running, S.W., 2006. Impacts of climate change on natural forest productivity - evidence since the middle of the 20th century. Glob. Change Biol. 12, 862–882.
Bergeron, Y., 2000. Species and stand dynamics in the mixed woods of Quebec's southern boreal forest. Ecology 81, 1500–1516.
Barnett, T.P., Adam, J.C., Lettenmaier, D.P., 2005. Potential impacts of a warming climate on water availability in snow-dominated regions. Nature 438, 303.
Campbell, D., Pollick, H.F., Lituri, K.M., Horowitz, A.M., Brown, J., Janssen, J.A., de la Torre, M.A., 2005. Improving the oral health of Alaska natives. Am. J. Public Health 95, 1880 1880–1880.
Crookston, N.L., Rehfeldt, G.E., Dixon, G.E., Weiskittel, A.R., 2010. Addressing climate change in the forest vegetation simulator to assess impacts on landscape forest dynamics. For. Ecol. Manage. 260, 1198–1211.
Daly, C., Halbleib, M., Smith, J.I., Gibson, W.P., Doggett, M.K., Taylor, G.H., Curtis, J., Pasteris, P.P., 2008. Physiographically sensitive mapping of climatological temperature and precipitation across the conterminous United States. Int. J. Climatol. 28, 2031–2064.
Diebold, F.X., Ohanian, L.E., Berkowitz, J., 1998. Dynamic equilibrium economies: A framework for comparing models and data. Rev. Econ. Stud. 65, 433–451.
Dixon, G., Johnson, R.R., Schroeder, D., 1992. Southeast Alaska/coastal British Columbia (SEAPROG) Prognosis Variant of the Forest Vegetation Simulator. Timber Management Service Center, Forest Service, US Department of Agriculture, Fort Collins CO.
Dale, V.H., Joyce, L.A., McNulty, S., Neilson, R.P., Ayres, M.P., Flannigan, M.D., Hanson, P.J., Irland, L.C., Lugo, A.E., Peterson, C.J., Simberloff, D., 2001. Climate change and forest disturbances: climate change can affect forests by altering the frequency, intensity, duration, and timing of fire, drought, introduced species, insect and pathogen outbreaks, hurricanes, windstorms, ice storms, or landslides. AIBS Bulletin 51, 723–734.
Desprez-Loustau, M.L., Marcais, B., Nageleisen, L.M., Piou, D.A., Vannini, A., 2006. Interactive effects of drought and pathogens in forest trees. Ann. For. Sci. 63, 597–612.
Dyrness, C.T., 1980. White spruce. In: Eyre, F.H. (Ed.), Forest Cover Types of the United States and Canada. Society of American Foresters, Washington, DC, pp. 81.
Fischer, A., Marshall, P., Camp, A., 2013. Disturbances in deciduous temperate forest ecosystems of the northern hemisphere: their effects on both recent and future forest development. Biodivers. Conserv. 22, 1863–1893.
Ford, E.D., Deans, J.D., 1978. The effects of canopy structure on stemflow, throughfall and interception loss in a young Sitka spruce plantation. J. Appl. Ecol. 15, 905–917.
Hernandez, R.E., Bustos, C., Fortin, Y., Beaulieu, J., 2001. Wood machining properties of white spruce from plantation forests. For. Prod. J. 51, 82.
Hansen, A.J., Neilson, R.P., Dale, V.H., Flather, C., Iverson, L., Currie, D.J., Bartlein, P., 2001. Global change in forests: responses of species, communities, and biomes. Bioscience 51, 765–779.
IPCC, 2013 Summary for policymakers. In: climate change 2013: the physical science basis. Contribution of Working Group I to the Fifth Assessment Report of the Intergovernmental Panel on Climate Change Cambridge University Press, Cambridge, United Kingdom and New York, NY, USA.
Juday, G.P., Ott, R.A., Valentine, D.W., Barber, V.A., 1998. Forests, climate stress, insects, and fire. Implications of Global Change in Alaska and the Bering Sea Region, Center for Global Change and Arctic System Research, University of Alaska Fairbanks, Fairbanks, Alaska, USA, pp. 23–49.
Juday, G.P., Barber, V.A., Duffy, P., 2005. Forests, land management, and agriculture. In: Symon, C., Arris, L., Heal, B. (Eds.), Arctic Climate Impact Assessment. Cambridge University Press, New York, NY, pp. 781–862.
Keyser, C.E., 2008. Southeast Alaska and coastal British Columbia (AK) variant overview—forest vegetation simulator. Internal Report. USDA Forest Service, Forest Management Service Center, Fort Collins, Colorado.
Kramer, M.G., Hansen, A.J., Taper, M.L., Kissinger, E.J., 2001. Abiotic controls on long-term windthrow disturbance and temperate rain forest dynamics in southeast Alaska. Ecology 82, 2749–2768.
Kirkland, J., Barrett, T., 2016. Colossal carbon! Disturbance and biomass dynamics in Alaska's national forests. Science Findings 182. US Department of Agriculture, Forest Service, Pacific Northwest Research Station, Portland, OR. 5 p., 182.
Liang, J., Picard, N., 2013. Matrix model of forest dynamics: An overview and outlook. For. Sci. 59, 359–378.
Liang, J., Zhou, M., Verbyla, D.L., Zhang, L., Springsteen, A.L., Malone, T., 2011. Mapping forest dynamics under climate change: A matrix model. For. Ecol. Manag. 262, 2250–2262.
Liang, J., Zhou, M., 2014. Large-scale geospatial mapping of forest carbon dynamics. J. Sustain. For. 33, 104–122.
Liang, J., Buongiorno, J., Monserud, R.A., 2005. Growth and yield of all-aged Douglas-fir western hemlock forest stands: a matrix model with stand diversity effects. Can. J. For. Res. 35, 2368–2381.
Lennon, J., Kunin, W., Corne, S., Carver, S., Van, H.W., 2002. Are Alaskan trees found in locally more favourable sites in marginal areas? Glob. Ecol. Biogeogr. 11, 103–114.
Liang, J., Buongiorno, J., Monserud, R.A., Kruger, E.L., Zhou, M., 2007. Effects of diversity of tree species and size on forest basal area growth, recruitment, and mortality. For. Ecol. Manage. 243, 116–127.
Liang, J., Buongiorno, J., Monserud, R.A., 2006. Bootstrap simulation and response surface optimization of management regimes for Douglas-fir/western hemlock stands. For. Sci. 52, 579–594.
Lertzman, K.P., Sutherland, G.D., Inselberg, A., Saunders, S.C., 1996. Canopy gaps and the landscape mosaic in a coastal temperate rain forest. Ecology 77, 1254–1270.
Liang, J., 2010. Dynamics and management of Alaska boreal forest: An all-aged multi-species matrix growth model. For. Ecol. Manage. 260, 491–501.
Latta, G., Temesgen, H., Adams, D., Barrett, T., 2010. Analysis of potential impacts of climate change on forests of the United States Pacific Northwest. For. Ecol. Manage. 259, 720–729.
Macdonald, E., Hubert, J., 2002. A review of the effects of silviculture on timber quality of Sitka spruce. Forestry 75, 107–138.
Millenium Ecosystem Assessment, 2005. Ecosystems and Human Well-Being: Synthesis. Island Press, Washington, DC, pp. 126.
McClellan, M.H., Swanston, D.N., Hennon, P.E., Deal, R.L., De Santo, T.L., Wipfli, M.S., 2000. Alternatives to clearcutting in the old-growth forests of southeast Alaska: study plan and establishment report. United States department of agriculture forest service general technical report.
Meyer, W.H., 1937. Yield of even-aged stands of Sitka spruce and western hemlock (No. 165657). United States Department of Agriculture, Economic Research Service.
McClellan, M.H., 2005. Recent research on the management of hemlock–spruce forests in southeast Alaska for multiple values. Landsc. Urban Plan. 72, 65–78.
Ma, W., Liang, J., Cumming, J.R., Lee, E., Welsh, A.B., Watson, J.V., Zhou, M., 2016. Fundamental shifts of central hardwood forests under climate change. Ecol. Model. 332, 28–41.
Ma, W., Zhou, M., 2017. Assessments of harvesting regimes in central hardwood forests under climate and fire uncertainty. For. Sci. 64, 57–73.
Ma, W., Domke, G.M., D'Amato, A.W., Woodall, C.W., Walters, B.F., Deo, R.K., 2018a. Using matrix models to estimate aboveground forest biomass dynamics in the eastern USA through various combinations of LiDAR, Landsat, and forest inventory data. Environ. Res. Lett. 13, 125004.
Ma, W., Woodall, C.W., Domke, G.M., D'Amato, A.W., Walters, B.F., 2018b. Stand age versus tree diameter as a driver of forest carbon inventory simulations in the northeastern US. Can. J. For. Res. 48, 1–13.
Mason, B., Perks, M.P., 2011. Sitka spruce (Picea sitchensis) forests in Atlantic Europe: changes in forest management and possible consequences for carbon sequestration. Scand. J. Forest Res. 26, 72–81.
Nowacki, G.J., Spencer, P., Fleming, M., Brock, T., Jorgenson, T., 2003. Unified ecoregions of Alaska: 2001 (No. 2002-297). Geological Survey (US).
Namaalwa, J., Eid, T., Sankhayan, P., 2005. A multi-species density-dependent matrix growth model for the dry woodlands of Uganda. For. Ecol. Manag. 213, 312–327.
Ping, C.L., Michaelson, G.J., Kimble, J.M., 1997. Carbon storage along a latitudinal transect in Alaska. Nutr. Cycl. Agroecosys. 49, 235–242.
Peterson, R.L., Liang, J., Barrett, T.M., 2014. Modeling population dynamics and woody biomass in Alaska coastal forest. For. Sci. 60, 391–401.
Picard, N., Bar-Hen, A., Guédon, Y., 2003. Modelling diameter class distribution with a second-order matrix model. For. Ecol. Manage. 180, 389–400.
Pielou, E., 1977. Mathematical Ecology. John Wiley & Sons, New York.
Pretzsch, H., Biber, P., Schütze, G., Uhl, E., Rötzer, T., 2014. Forest stand growth dynamics in Central Europe have accelerated since 1870. Nat. Commun. 5.
Ruess, R.W., Hendrick, R.L., Bryant, J.P., 1998. Regulation of fine root dynamics by mammalian browsers in early successional Alaskan taiga forests. Ecology 79, 2706–2720.
Ritchie, M.W., 1999. A Compendium of Forest Growth and Yield Simulators for the Pacific Coast States. US Department of Agriculture, Forest Service, Pacific Southwest Research Station.
Runkle, D.E., 1987. Vector autoregressions and reality. J. Bus. Econ. Stat. 5, 437–442.
Rupp, T.S., 2008. Projected vegetation and fire regime response to future climate change in Alaska. In: . Preliminary Report prepared for U.S. Fish and Wildlife Service National Wildlife Refuge System. University of Alaska Fairbanks, Fairbanks, AK, pp. 22.
Swann, A.L., Fung, I.Y., Levis, S., Bonan, G.B., Doney, S.C., 2010. Changes in Arctic vegetation amplify high-latitude warming through the greenhouse effect. Proc. Natl. Acad. Sci. 107, 1295–1300.
Stier, J.C., 1980. Estimating the production technology in the US forest products industries. For. Sci. 26, 471–482.
Serreze, M.C., Walsh, J.E., Chapin, F.S., Osterkamp, T., Dyurgerov, M., Romanovsky, V., Oechel, W.C., Morison, J., Zhang, T., Barry, R.G., 2000. Observational evidence of recent change in the northern high-latitude environment. Clim. Change 46, 159–207.
Schoene, D.H.F., Bernier, P.Y., 2012. Adapting forestry and forests to climate change: A challenge to change the paradigm. For. Policy Econ. 24, 12–19.
Stokes, V., Lee, S., Forster, J., Fletcher, A., 2018. A comparison of Sitka spruce x white spruce hybrid families as an alternative to pure Sitka spruce plantations in upland Britain. Forestry 91, 650–661.

Taylor, R.F., 1934. Yield of Second-growth Western Hemlock-Sitka Spruce Stands in Southeastern Alaska. US Department of Agriculture.
Tobin, J., 1958. Estimation of relationships for limited dependent variables. Econometric. Soc. 26, 24–36.
van Hees, W.W., 2003. Forest resources of southeast Alaska, 2000: results of a single-phase systematic sample. Res. Pap. PNW-RP-557. US Department of Agriculture, Forest Service, Pacific Northwest Research Station, Portland, OR.
Zhou, M., Buongiorno, J., 2004. Nonlinearity and noise interaction in a model of forest growth. Ecol. Model. 180, 291–304.
Zhang, J., Huang, S., He, F., 2015. Half-century evidence from western Canada shows forest dynamics are primarily driven by competition followed by climate. Proc. Natl. Acad. Sci. 112, 4009–4014.
Zhou, M., Liang, J., Buongiorno, J., 2008. Adaptive versus fixed policies for economic or ecological objectives in forest management. For. Ecol. Manage. 254, 178–187.